JOURNAL OF MATERIALS SCIENCE 21 (1986) 4173–4178

Size effects and ductile–brittle transition of polypropylene

A. CARPINTERI
Istituto Scienza delle Costruzioni, University of Bologna, 40136 Bologna, Italy
C. MAREGA, A. SAVADORI
Zeltron, Istituto Zanussi per la Ricerca SpA, 33030 Campoformido, Udine, Italy

The influence of specimen width on fracture parameters has been investigated. The range examined was sufficiently large to obtain ductile and brittle fractures. With reference to previously published work, the phenomenology has been analysed by combining BCS model and Carpinteri's brittleness number approach.

Nomenclature

a	crack length
$f(a/W)$	shape function according to ASTM specification [16]
$F(a/W)$	shape function according to Tada Paris notation [21]
E	elastic modulus
K_{IC}	plane strain fracture toughness
K_{IC}^{f}	fictitious plane strain fracture toughness
K_{IC2}	plane stress fracture toughness
J_{IC}^{f}	J-integral at maximum load
L	span
$\overline{M_w}$	weight average molecular weight
$\overline{M_n}$	number average molecular weight
$\overline{M_w}/\overline{M_n}$	polydispersity
P_M	maximum load
P_F	load of brittle fracture
P_P	load of plastic collapse
s	brittleness number
V	machine cross speed
W	specimen width
σ_y	yield stress
$\dot{\varepsilon}$	strain rate

1. Introduction

One of the central of problems of fracture mechanics is to obtain correct data for fracture toughness (K_C), critical strain energy release rate G_C or crack opening displacement (COD) for design. Unfortunately, very often the values obtained on a laboratory scale cannot be applied in failure prediction of larger structures. Even though polymers are rarely involved in large structures, there is a necessity to have fracture intrinsic parameters also for these materials.

Results published to date on this subject have shown that [1–11]:

1. Specimen thickness influences the K_C values of polymers as well as those of metals: the thicker the specimen is, the lower the fracture toughness K_C results will be. On the other hand, a lower bound to K_C, named "plane strain fracture toughness" K_{IC}, does exist. The conditions (the same found for metals) to obtain K_{IC} are

$$B \geqslant 2.5\left(\frac{K_{IC}}{\sigma_y}\right)^2 \tag{1}$$

where B is the specimen thickness and σ_y is the yield stress in tension.

2. If the previous relationship is not fulfilled, but LEFM is still valid, K_{IC} can be obtained by extrapolation of the following formula

$$K_{IC}^{f} = K_{IC} + \frac{1}{B}\left[\frac{K_{IC}^2\,(K_{IC2}-K_{IC})}{\pi\sigma_y^2}\right] \tag{2}$$

where K_{IC}^{f} is the fictitious K_{IC} and K_{IC2} is the plane stress intensity factor.

The works of Chan and Williams [12] and Hashemi and Williams [13] show that the specimen width must be

$$W \geqslant 6.25\left(\frac{K_{IC}}{\sigma_y}\right)^2 \quad \text{or} \quad 5\left(\frac{K_{IC}}{\sigma_y}\right)^2 \tag{3}$$

If this relationship is not satisfied, but LEFM is still valid, K_{IC} can be derived using the Bilby–Cottrell–Swinden (BCS) model [13]. On the other hand, it remains unsolved to what extent it is possible to design against catastrophic failure based only on ductile data.

With reference to their previously published paper [14] the authors examine such a problem combining the BCS model and Carpinteri's brittleness number approach [15].

2. Experimental techniques

2.1. Materials

The material examined was a polypropylene homopolymer (PP). It was provided in slabs 100 cm × 200 cm × 4 cm. The main properties of this material are given in Table I. Three-point bend specimen were cut from the slabs (Fig. 1). The specimens were of different widths (0.5, 1, 2, 4, 8, 12 cm) and the same thickness (4 cm). The shape ratio was $L/W = 4$ where L is the span and W is the width. The loading velocity was controlled in order to obtain a constant strain rate $\dot{\varepsilon} = 0.001\ \text{sec}^{-1}$.

0022–2461/86 $03.00 + .12

TABLE I Physical characteristics of PP

Characteristics	Method	Unit	Data
$\overline{M_w}$	Light scattering	–	7.0×10^5
$\overline{M_w}/\overline{M_n}$	GPC	–	6.2
"Melt flow rate"	ASTM D 1238	10^{-1} g	0.46
Young modulus	ASTM D 790	$MN\,m^{-2}$	1400
Yield stress	ASTM D 638	$MN\,m^{-2}$	33
Density	ASTM D 1505	$cm^{-3}\,g$	0.912

The following formula was used [13]:

$$\dot{\varepsilon} = \frac{6VW}{L^2} \tag{4}$$

where V is the loading velocity or machine cross speed.

For each value of W, five different relative crack depths were utilized: $a/W = 0.1, 0.2, 0.3, 0.4. 0.5$. The tests were carried out at 23° C. Table II shows the types of loading curve obtained. Except for the larger specimens (width 12 cm), the fracture process was stable and very ductile, but no necking near the crack was noticed (Fig. 2). The plastic zone in front of crack tip had a linear shape.

2.2. Stress intensity factor

The fictitious fracture toughness was determined for all values of W according to the equation [16]

$$K_{IC}^{f} = \frac{P_M L}{BW^{3/2}} f(a/W)$$

$$f(a/W) = 2.9(a/W)^{1/2} - 4.6(a/W)^{3/2} + 2.18(a/W)^{5/2} \tag{5}$$

where P_M is the maximum load, $f(a/W)$ the shape factor according to ASTM specification and K_{IC}^{f} the fictitious K_{IC} (the material shows such a high ductility that LEFM cannot be correctly applied).

Table III shows the data obtained by this formula and Fig. 3 shows the variation plotted against the specimen width in comparison to K_{IC} data obtained by the J_{IC} approach. The procedure proposed by Rice *et al.* [17] was followed and the formula

$$K_{IC}^{f} = (J_{IC}^{f} E)^{1/2} \qquad (a/W = 0.5) \tag{6}$$

was used. The following considerations should be drawn from this data:

1. In both cases K_{IC}^{f} increases in a parabolic manner with W.
2. The K_{IC}^{f} values obtained from J_{IC}^{f} are higher than those from the ASTM formula.

This may be due not only to the fact that the crack advancement is calculated at maximum load (with $a/W = 0.5$ the error is minimum), but also to the uncorrected use of Equation 6, strictly valid in the linear elastic range.

TABLE II Types of experimental curves

W(cm)	$a\,W$	Curve
0.5	0.1	A
	0.2	A
	0.3	A
	0.4	A
	0.4	A
	0.5	A
1	0.1	A
	0.2	A
	0.3	A
	0.4	A
	0.5	A
2	0.1	A
	0.2	A
	0.3	A
	0.4	A
	0.5	A
4	0.1	A
	0.2	A
	0.3	A
	0.4	A
	0.5	A
8	0.1	B
	0.2	B
	0.3	B
	0.4	A
	0.5	A
12	0.1	C
	0.2	B
	0.3	B
	0.4	B
	0.4	A

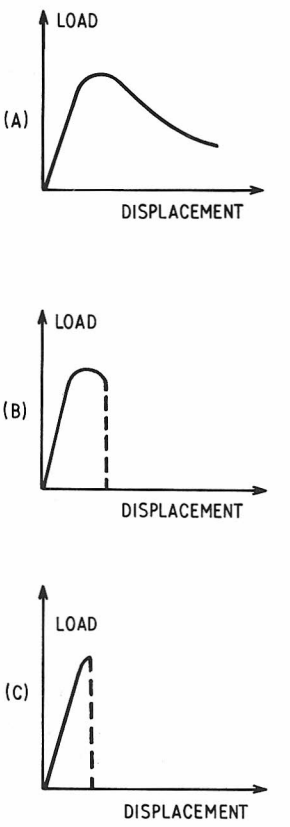

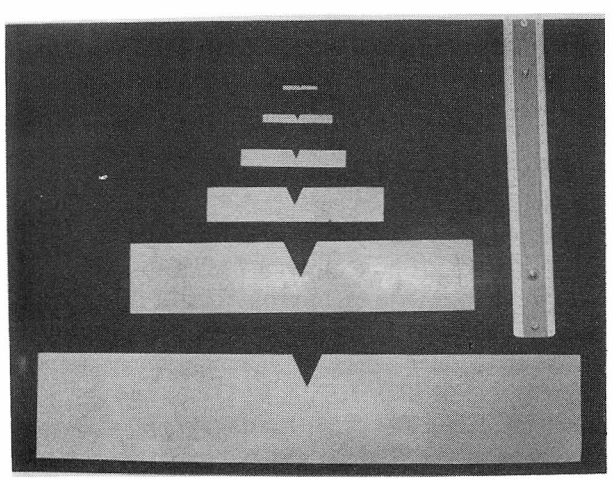

Figure 1 Different sizes of the tested specimens.

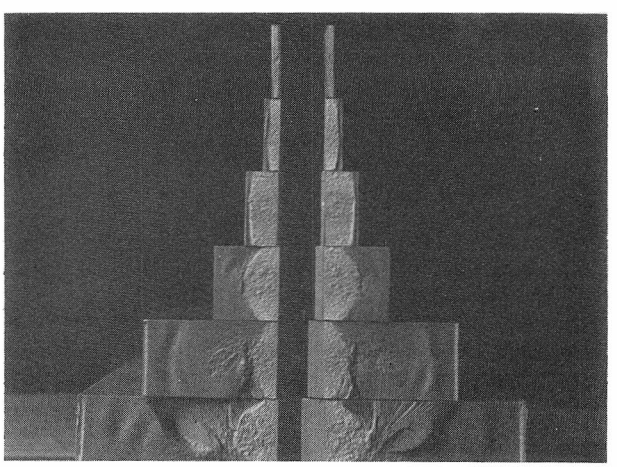

Figure 2 Different ratios between ductile and cleavage fracture when the specimen width varied.

TABLE III Experimental fracture mechanics parameters

W(cm)	a/W	J_{IC}^{f} (Rice *et al.* [17]) (kJ m^{-2})	$K_{IC}^{f} = (J_{IC}^{f}E)^{1/2}$ (MN m$^{-3/2}$)	K_{IC}^{f} (ASTM) (MN m$^{-3/2}$)	Ave.
0.5	0.1	–	–	2.61	2.10
	0.2	–	–	2.03	
	0.3	–	–	2.00	
	0.4	–	–	1.95	
	0.5	8.54	3.48	1.89	
1.0	0.1	–	–	2.28	2.48
	0.2	–	–	2.57	
	0.3	–	–	2.59	
	0.4	–	–	2.66	
	0.5	10.00	3.58	2.32	
2.0	0.1	–	–	3.05	3.15
	0.2	–	–	3.22	
	0.3	–	–	3.26	
	0.4	–	–	3.25	
	0.5	10.63	3.88	2.98	
4.0	0.1	–	–	3.62	3.63
	0.2	–	–	3.73	
	0.3	–	–	3.78	
	0.4	–	–	3.63	
	0.5	14.40	4.51	3.41	
8.0	0.1	–	–	4.39	4.50
	0.2	–	–	4.73	
	0.3	–	–	4.71	
	0.4	–	–	4.41	
	0.5	23.37	5.75	4.26	
12.0	0.1	–	–	5.33	5.19
	0.2	–	–	5.41	
	0.3	–	–	5.35	
	0.4	–	–	5.01	
	0.5	30.17	6.53	4.83	

3. Size scale transition from plastic flow collapse to brittle crack propagation

Owing to the different physical dimensions of strength $[FL^{-2}]$ and fracture toughness $[FL^{-3/2}]$, scale effects are always present in the usual fracture testing of common engineering materials. This means that for the usual size of the laboratory specimens, the ultimate strength collapse or the plastic collapse at the ligament tends to anticipate the real crack propagation collapse [15]. Such competition between collapses of a different nature can be easily proved by considering the ASTM formula for the three-point bending test evaluation of fracture toughness [16]:

$$K_I = \frac{PL}{BW^{3/2}} f(a/W) \tag{7a}$$

Under crack propagation conditions, Equation 7a

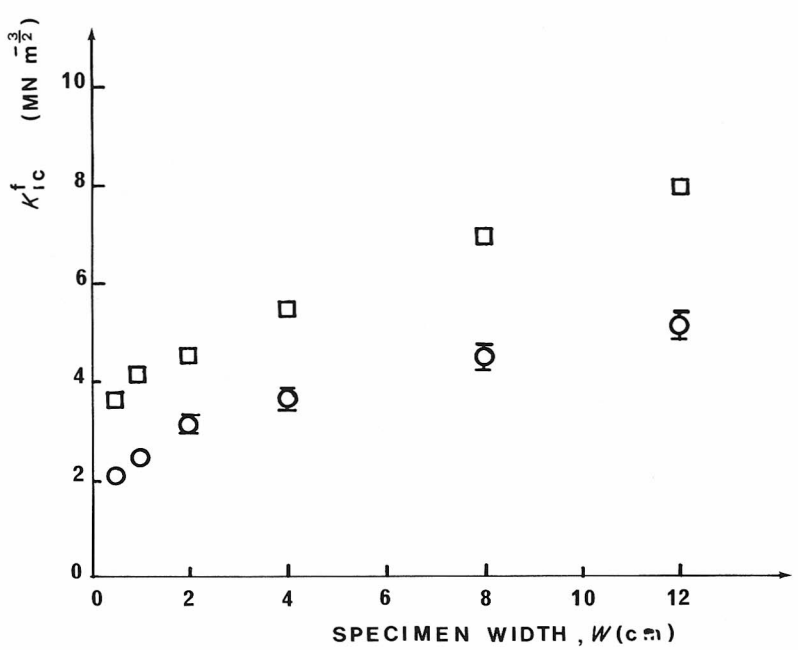

Figure 3 Fracture toughness K_{IC}^{f} plotted against specimen width W. (□) Rice *et al.* [17], (○) [16].

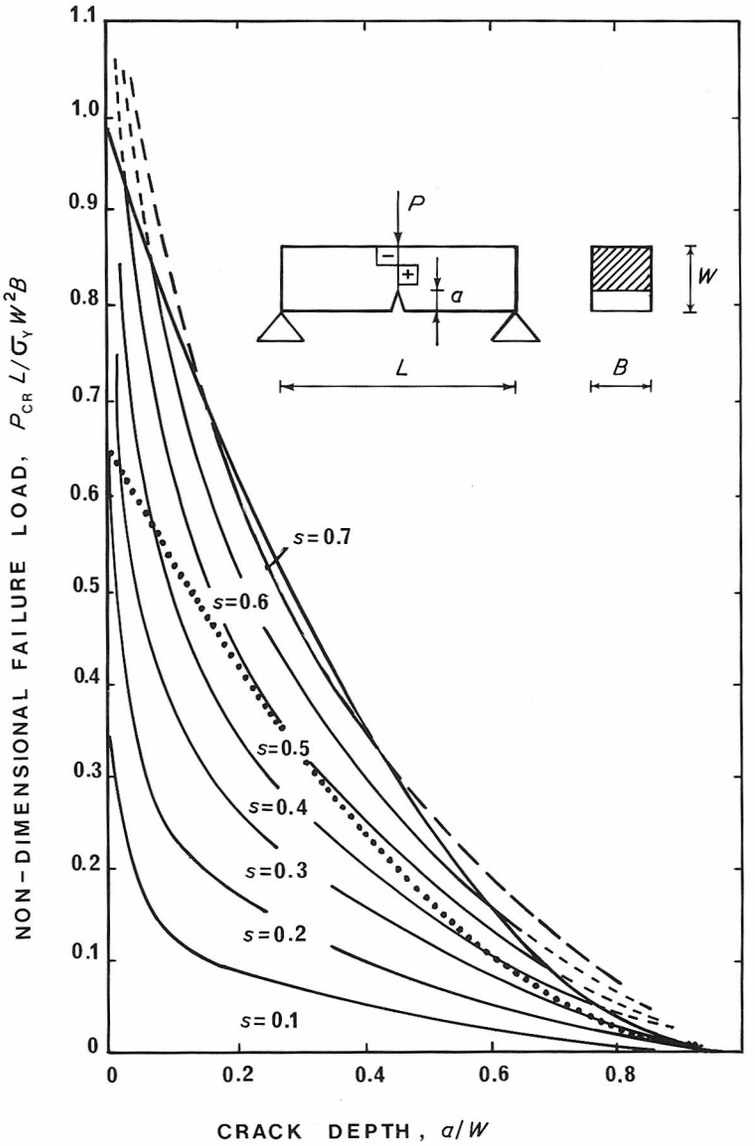

Figure 4 Interaction between crack propagation and plastic hinge formation at the ligament. —— Plastic flow collapse (elastic–perfectly plastic material); ····· ultimate strength collapse (elastic–brittle material). $s = K_{IC}/\sigma_y W^{1/2}$.

becomes:

$$K_{IC} = \frac{P_F L}{BW^{3/2}} f(a/W) \tag{7b}$$

where P_F is the external load of brittle fracture. If both members of Equation 7b are divided by $\sigma_y W^{1/2}$ we obtain:

$$\frac{K_{IC}}{\sigma_y W^{1/2}} = s = \frac{P_F L}{\sigma_y BW^2} f(a/W) \tag{8}$$

where s is a dimensionless number able to describe the brittleness of the specimen.

Rearranging Equation 8 gives:

$$\frac{P_F L}{\sigma_y BW^2} = \frac{s}{f(a/W)} \tag{9}$$

On the other hand, it is possible to consider the non-dimensionless load of plastic hinge formation at the ligament:

$$\frac{P_P L}{\sigma_y BW^2} = \left(1 - \frac{a}{W}\right)^2 \tag{10}$$

Equations 9 and 10 are plotted in Fig. 4 as functions of the crack depth a/W. While the former produces a family of curves by varying the brittleness number s, the latter is represented by a unique curve. It is easy to realize that plastic collapse precedes crack propagation for each crack depth when the brittleness number is higher than the critical value $s_0 = 0.75$. For lower values of s plastic collapse anticipates crack propagation only for crack depths external to a certain interval. This means that real fracture phenomena occur only for sufficiently low fracture toughnesses, high yield strengths and/or large structural sizes. The individual values of K_{IC}, σ_y and W are of no significance. What is important is their function s.

Recalling Equations 9 and 10, we can obtain the ratio between fictitious and real fracture toughness, which is equal to the ratio between load of plastic collapse, P_P, and load of crack propagation, P_F, when $P_P < P_F$, and equal to unity when $P_P > P_F$:

$$\frac{K_{IC}^f}{K_{IC}} = \frac{P_P}{P_F} = \frac{1}{s}\left(1 - \frac{a}{W}\right)^2 f(a/W) \quad \text{for } P_P < P_F \tag{11a}$$

$$\frac{K_{IC}^f}{K_{IC}} = 1 \quad \text{for } P_P > P_F \tag{11b}$$

Combining the definitions of brittleness number,

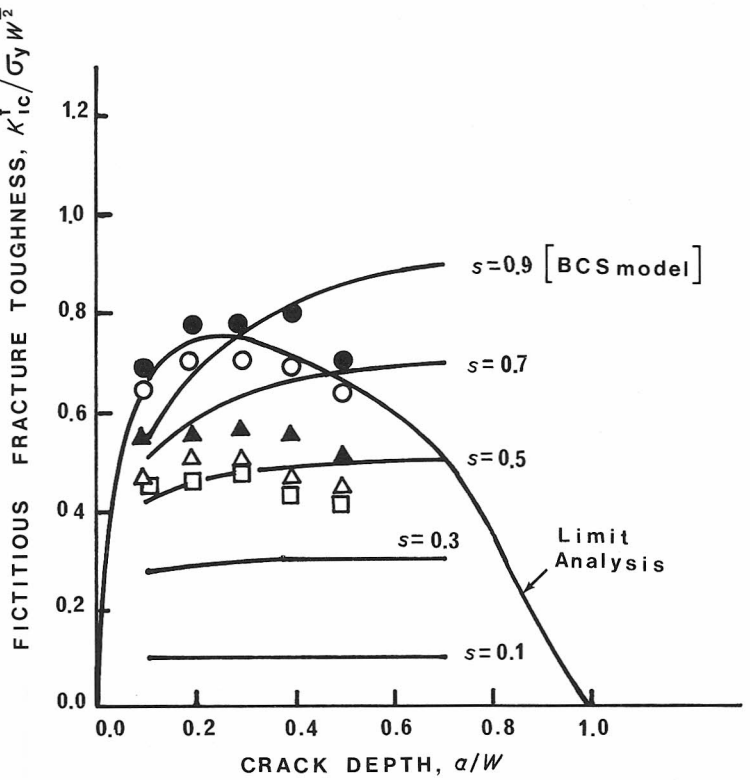

Figure 5 Fictitious fracture toughness plotted against crack depth. W = (●) 1 cm; (○) 2 cm; (▲) 4 cm; (△) 8 cm; (□) 12 cm.

Equations 8 and 11, we obtain:

$$\frac{K^f_{IC}}{\sigma_y W^{1/2}} = \left(1 - \frac{a}{W}\right)^2 f(a/W) \qquad \text{for } P_P < P_F \tag{12a}$$

$$\frac{K^f_{IC}}{\sigma_y W^{1/2}} = s \qquad \text{for } P_P > P_F \tag{12b}$$

Equation 12a is represented in Fig. 5 as a bell-shaped curve vanishing for $a/W = 0$ and $a/W = 1$. It presents a maximum for that value of a crack depth for which the fracture curve $s = s_0$ is tangent to the plastic flow curve in Fig. 4. More precisely, for $s > s_0$ Equation 12a is valid for each crack depth a/W, whereas for $s < s_0$ Equation 12a is valid for external crack depths and Equation 12b for central crack depths. Equation 12a is also represented in Fig. 6 by varying the specimen depth W. The dark shaded area is where the curves $a/W = 0.1$ to $a/W = 0.5$ are concentrated. It is a very narrow strip, especially for smaller values of W.

When $s > s_0$, the parabola (Equation 12a) is

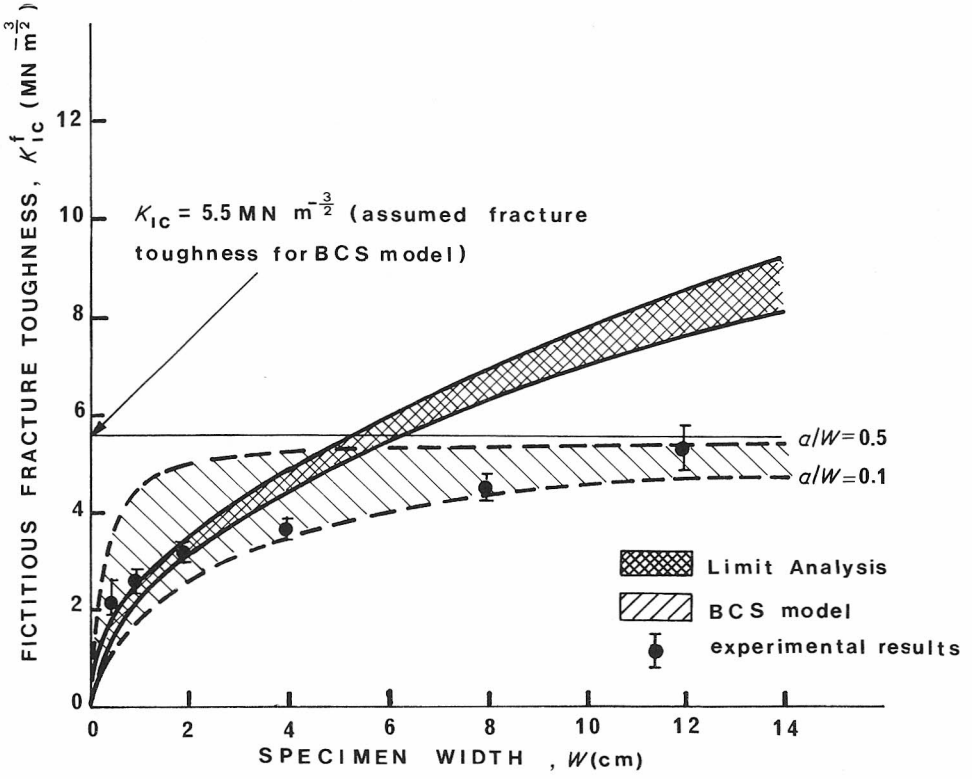

Figure 6 Fictitious fracture toughness plotted against specimen width.

replaced by the horizontal straight line $K_{IC}^{f} = K_{IC}$. The experimental points present a course which is only initially similar to that of Equation 12a. This means that, only for small specimens (W = 0.5, 1.0 or 2.0 cm) the collapse can be exactly described by a plastic flow at the ligament.

By increasing the size scale a transition from plastic flow occurs towards a true LEFM collapse. For W = 12 cm, however, the latter has not yet been reached, since the experimental points are still ascending. It is difficult to predict the true value of fracture toughness exactly. On the other hand, if experimental work was carried out on larger specimens, it would be possible to standardize an extrapolation technique with a smaller number of specimens. An attempt is made to describe the ductile–brittle transition through the BCS–cohesive crack model [18].

The following expression for the fictitious fracture toughness is assumed:

$$K_{IC}^{f} = \sigma_f (\pi a)^{1/2} F(a/W) \quad (13)$$

where σ_f is the nominal stress at failure and F is the shape-function in the Tada–Paris notation [19]. If we recall the equivalence:

$$F(a/W) = \frac{2f(a/W)}{3(\pi a/W)^{1/2}} \quad (14)$$

between the Tada–Paris function and the ASTM function, the BCS fracture toughness:

$$K_{IC}^{f} = (\pi a)^{1/2} F(a/W) \frac{2}{\pi} \sigma_y \times \cos^{-1} \left\{ \exp - \left[\frac{\pi K_{IC}^2}{8\sigma_y^2 a F(a/W)} \right] \right\} \quad (15)$$

is transformed as follows:

$$\frac{K_{IC}^{f}}{\sigma_y W^{1/2}} = \frac{4}{3\pi} f(a/W) \cos^{-1} \left\{ \exp - \frac{9\pi^2 s^2}{32 f^2 (a/W)} \right\} \quad (16)$$

Equation 16 is plotted in Fig. 5 as a function of crack depth a/W and varying the brittleness number s. The experimental points are on the limit analysis curve for W = 1 and 2 cm, whereas they fall below it for larger specimens.

Equation 16 is also represented in Fig. 6. According to the BCS model it is necessary to assume a true K_{IC} value to be inserted into Equation 16. The value $K_{IC} = 5.5\,MN\,m^{-3/2}$ is that which best fits the experimental results.

The family of curves a/W = 0.1 to a/W = 0.5 is more spread for small than for large sizes in this case. The opposite occurs for the limit analysis prediction. It is very clear from Fig. 6 that a simple plastic collapse at the ligament occurred for small size scales (W = 0.5, 1.0, 2.0 cm), whereas the transition from plastic collapse to brittle fracture is satisfactorily captured by the BCS model, especially for shallow cracks (W = 4.0, 8.0 cm).

References

1. J. G. WILLIAMS and M. PARVIN, *Int. Fract.* **11** (1975) 963.
2. *Idem, J. Mater. Sci.* **10** (1975) 1883.
3. Y. W. MAY and J. G. WILLIAMS, *ibid.* **12** (1977) 1376.
4. R. A. GLEDHIL and A. J. KINLOCH, *Prop. Exp.* **4** (1979) 73.
5. S. Y. HOBBS and R. C. BOPP, *Polymer* **21** (1980) 559.
6. P. L. FERNANDO and J. G. WILLIAMS, *Polym. Eng. Sci.* **20** (1980) 215.
7. R. A. GLEDHIL and A. J. KINLOCH, *J. Spacecrafts Rockets* **18** (1981) 333.
8. P. L. FERNANDO and J. G. WILLIAMS, *Polym. Eng. Sci.* **21** (1980) 1003.
9. J. HODGKINSON, A. SAVADORI and J. G. WILLIAMS, *J. Mater. Sci.* **18** (1983) 2319.
10. H. HOFFMANN, W. GRELLMANN, E. HILLE and R. NEWE, *Plast. Kautschuck* **29** (1982) 230.
11. A. SANDT, *Kunstoffe* **12** 791.
12. M. K. V. CHAN and J. G. WILLIAMS, *Polym. Eng. Sci.* (1981) 1019.
13. S. HASHEMI and J. G. WILLIAMS, *J. Mater. Sci.* **19** (1984) 3746.
14. A. CARPINTERI, C. MAREGA and A. SAVADORI, *Eng. Fract. Mech.* **21** (1985) 263.
15. A. CARPINTERI, *ibid.* **16** (1982) 467.
16. "Standard Method of Test for Plane Strain Fracture Toughness of Metallic Materials", ASTM E 399-74 (American Society for Testing and Materials, Philadelphia, Pennyslvania, 1974).
17. J. R. RICE, P. C. PARIS and J. G. MERKLE, ASTM STP 536 (American Society for Testing and Materials, Philadelphia, Pennyslvania, 1973) p. 231.
18. B. A. BILBY, A. H. COTTRELL and K. H. SWINDEN, *Proc. Roy Soc. (London)* **A272** (1963) 304.
19. H. TADA, P. PARIS and G. IRWIN, "The stress Analysis of Crack Handbook" (Del Res. Corp., St. Louis, 1963).

Received 31 July 1985
and accepted 11 February 1986